Acta Neuropathologica
https://doi.org/10.1007/s00401-022-02403-w

REVIEW

Consequences of variability in α-synuclein fibril structure on strain biology

Sara A. M. Holec[1] · Samantha L. Liu[1,2] · Amanda L. Woerman[1]

Received: 5 January 2022 / Revised: 26 January 2022 / Accepted: 27 January 2022

Abstract

Synucleinopathies are a group of clinically and neuropathologically distinct protein misfolding diseases caused by unique α-synuclein conformations, or strains. While multiple atomic resolution cryo-electron microscopy structures of α-synuclein fibrils are now deposited in Protein Data Bank, significant gaps in the biological consequences arising from each conformation have yet to be unraveled. Mutations in the α-synuclein gene (*SNCA*), cofactors, and the solvation environment contribute to the formation and maintenance of each disease-causing strain. This review highlights the impact of each of these factors on α-synuclein misfolding and discusses the implications of the resulting structural variability on therapeutic development.

Keywords α-synuclein · Multiple system atrophy · Parkinson's disease · Strains · Synucleinopathies

Introduction

A-synuclein is a 140-amino acid protein expressed predominantly in the nucleus and presynaptic terminals of neurons throughout the central nervous system with little to no expression in oligodendrocytes [5, 22, 72]. While its exact function in neurons is uncertain, data suggest α-synuclein plays a role in regulating synaptic vesicle exocytosis and endocytosis, neurotransmitter release, and SNARE complex formation [17, 31, 63, 75, 103, 104]. Burré et al. reported that α-synuclein interacts directly with synaptobrevin-2/VAMP2 within the SNARE complex, promoting its assembly by binding to and clustering synaptic vesicles, as well as facilitating their subsequent fusion to the presynaptic membrane [17]. Similarly, studies evaluating α-synuclein expression levels suggest it is involved in regulating exocytotic events in neurons [63, 75]. Structural studies indicate that the N-terminal tail of α-synuclein binds to acidic lipids, allowing for the formation of two α-helices joined by a linker, which aids its role as a chaperone for vesicle docking [18, 19, 26, 28, 47]. However, because α-synuclein is an intrinsically disordered protein, it can adopt a variety of conformations when not membrane-bound, including β-sheet-rich structures that initiate a protein misfolding cascade. The ability of α-synuclein to self-template misfolding, also known as the prion mechanism, underlies a group of neurodegenerative disorders termed synucleinopathies.

Synucleinopathies are movement disorders that vary both in clinical presentation and neuropathology. As a result, they are often subcategorized into two main groups. In the first, α-synuclein accumulates into Lewy bodies (LBs) and Lewy neurites (LNs) in neurons in Parkinson's disease (PD), dementia with Lewy bodies (DLB), and Parkinson's disease with dementia (PDD) patients [30, 94]. As a group, Lewy body disease (LBD) patients are typically diagnosed in their 60 s or at a later age and live up to two decades with supportive care [4]. PD is characterized by a resting tremor, gait abnormalities, and muscle stiffness [79]. In both PDD and DLB, parkinsonism is accompanied by dementia, but diagnosis depends on the timing of dementia onset relative to motor symptoms. In PDD patients, dementia develops after motor impairment, while dementia onset precedes the motor signs in DLB patients. Consistent with this variation in symptoms, LBD patients exhibit differences in LB and LN distribution; PD patients typically show LB distribution throughout the brainstem, substantia nigra, and basal ganglia, whereas cortical LBs are seen in PDD and DLB patients [13, 68]. In the second category of synucleinopathies, multiple system atrophy (MSA) is characterized by α-synuclein

✉ Amanda L. Woerman
awoerman@umass.edu

[1] Department of Biology, Institute for Applied Life Sciences, University of Massachusetts Amherst, Amherst, MA, USA

[2] Present Address: Molecular and Cellular Biology Program, Dartmouth College, Hanover, NH, USA

Published online: 04 February 2022

accumulating into glial cytoplasmic inclusions (GCIs) in oligodendrocytes and, to a lesser extent, neuronal cytoplasmic inclusions in neurons [78]. MSA patients are typically diagnosed in their 50–60 s and survive about 6–10 years following the onset of symptoms, which include cerebellar ataxia and idiopathic orthostatic hypotension [38–40]. MSA can be further subdivided based on the predominant clinical signs. In the cerebellar (MSA-C) subtype, patients develop tremors, oculomotor dysfunction, and ataxia, whereas in the parkinsonian (MSA-P) subtype, patients develop rigidity and nystagmus [40]. Notably, these differences in presenting symptoms coincide with differences in GCI distribution between the two subtypes [52].

While both LBDs and MSA are defined by α-synuclein pathology, to date, point mutations in the α-synuclein gene, *SNCA*, are only linked to LBD patients. The first mutation discovered in *SNCA* was the A53T mutation in the Contursi kindred [81]. This was shortly followed by the A30P and E46K mutations [51, 112]. More recently, known LBD-causing point mutations expanded to include A30G, H50Q, G51D, A53E, A53V, and T72M [3, 29, 55, 62, 80, 111]. Notably, two of these mutations, G51D and A53E, were reported in patients with neuropathological inclusions reminiscent of GCIs in addition to classical LB pathology [48, 80].

Applying the strain hypothesis to synucleinopathies

The ability of α-synuclein to give rise to several distinct neurological disorders is reminiscent of the finding that misfolding of the prion protein (PrP) is the underlying cause of a variety of prion diseases. While this finding was initially perplexing, the ability of an agent lacking a nucleic acid sequence to encode disease-specific information was explained by the *strain hypothesis*. The strain hypothesis proposes that the misfolded protein conformation determines which disease a patient will develop [8, 98]. In prion diseases, the kinetics of PrP mis-folding into each disease-causing conformation typically translates into strain-specific differences in disease onset and length of disease. Moreover, substantial data indicate that prion strains give rise to distinct neuropathological profiles in the brain (reviewed in [8, 14]). For example, while some PrP prion strains target the cerebellum, others have a larger impact on the cerebral cortex [16, 32]. This strain-specific selective vulnerability manifests as unique clinical presentations in affected individuals. As a result, each prion disease is defined and diagnosed by both distinct clinical and neuropathological features. Consistent with these observations, differences in the type and distribution of α-synuclein inclusions, as well as the associated clinical signs, strongly argue that discrete α-synuclein strains give rise to each synucleinopathy (reviewed in [45]). This hypothesis is bolstered by recent cryo-electron microscopy (cryo-EM) data from Schweighauser et al., while the authors resolved the structures of α-synuclein isolated from MSA patient samples, the lack of twist in filaments isolated from DLB patient samples impeded determination of the misfolded structure [92]. We discuss the biochemical, cellular, and animal data that point to the presence of distinct α-synuclein strains in LBD and MSA patient samples in a previous review article [45].

Over the last 6 years, several structures of misfolded α-synuclein have been resolved using a variety of fibril sources and imaging methods. In most cases, the combination of using recombinant protein, rather than patient-derived fibrils, along with the lack of a thorough biochemical and biological analysis accompanying each reported fibril structure, limits the conclusions we can draw about the strain-specific behavior associated with each conformation. This, in turn, constrains our ability as a field to determine what specific structural differences are responsible for dictating α-synuclein strain biology. For example, in this review, we offer a comprehensive discussion of the α-synuclein cryo-EM structures reported to date, with an emphasis on the effect of *SNCA* point mutations on α-synuclein conformation and misfolding kinetics. However, we are limited in our ability to pair these analyses with experimental or clinical data given the absence of robust biological profiles for each reported structure, as well as the lack of structures reported from synucleinopathy patients harboring *SNCA* mutations. This review also focuses on the clinical implications that may arise if we fail to prioritize the use of disease-relevant conformations to guide diagnostic and therapeutic development.

Structural diversity among α-synuclein fibrils

Unique sequence features contribute to amyloid structure

The amino acid sequence of α-synuclein is characterized by three general interaction domains: the N-terminal region (residues 1–60), the non-amyloid-β component (NAC; residues 61–96), and the C-terminal domain (residues 97–140; Fig. 1a). In addition, the portion of the N-terminal domain immediately preceding the NAC domain is commonly referred to as the preNAC region. While there is some variability in the amino acid residues that define the preNAC region, it is typically reported to include residues 47–54 at a minimum. The N-terminal and NAC domains contain seven imperfect repeats of the consensus sequence KTKEGV (residues 7–87), forming the amphipathic α-helices of the lipid-binding domain in which all known familial LBD mutations are located [7,

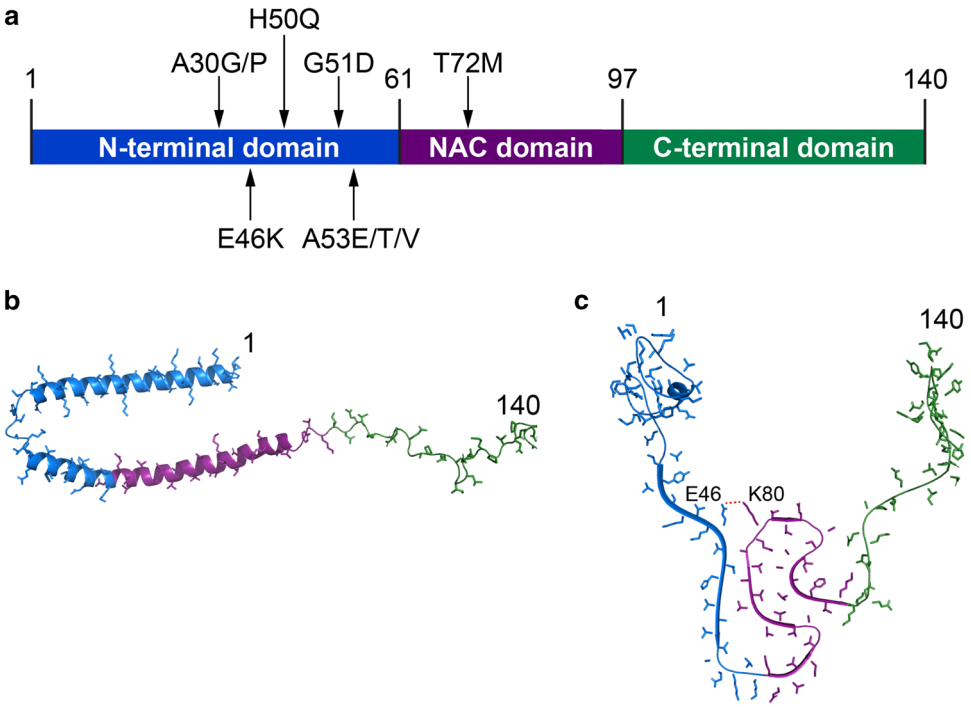

Fig. 1 The N-terminal NAC domain contributes to the α-synuclein fibril core. **a** A-synuclein is a 140-amino acid protein containing three general domains: the N-terminal domain (residues 1–61; blue), the NAC domain (residues 61–97; purple), and the C-terminal domain (residues 97–140; green). The majority of the reported familial Parkinson's disease mutations in α-synuclein, indicated with arrows, are located in the N-terminal domain. **b** Micelle-bound α-synuclein consists of two α-helices connected via a linker sequence, and a disordered C-terminal domain (PDB ID 1XQ8, [102]). **c** Solid-state NMR structure of WT recombinant full-length α-synuclein revealed a fibril core containing a Greek key motif that is stabilized by a salt bridge between residues E46 and K80 (dotted red line). This structured region of the protein fibril is flanked by an unstructured "fuzzy coat" region on the N- and C-termini (PDB ID 2N0A, [100])

21, 101]. The extension of the imperfect repeats into the hydrophobic NAC region is necessary for fibril formation, enabling the tight packing seen in the amyloid state [37]. In comparison, the C-terminus is enriched with acidic residues and prolines that yield a disordered and flexible domain. These sequence elements are easily observed in the nuclear magnetic resonance (NMR) structure described by Ulmer et al. in 2005 (Fig. 1b) [102]. Notably, the distinct charge differences between the N- and C-terminal regions of α-synuclein enable the structure to be highly dependent on the protein's environment [1, 10, 84, 109]. Finally, α-synuclein contains 18 glycine residues, amounting to ~ 13% of the total amino acid sequence (Table 1). The side chain, or R group, of a given amino acid introduces steric hindrance around the C_α carbon, which ultimately dictates how much strain each bond can tolerate and the conformations each residue can adopt. Glycine, with a hydrogen side chain, exhibits minimal conformational restriction on protein folding. The slight increase in glycine content in the α-synuclein sequence compared to other non-amyloid forming SNARE complex proteins (Table 1), along with the presence of the imperfect repeats, is thought to increase the flexibility of the protein, as well as contribute to its intrinsically disordered nature. As a consequence of this increase in conformational flexibility, the energy required for α-synuclein to adopt an amyloid conformation is lowered, increasing the capacity of α-synuclein to adopt a large number of amyloid conformations.

Table 1 Glycine content of SNARE complex proteins

Protein	Number of glycines	Sequence length	Percent glycines
α-synuclein	18	140	12.9
VAMP family	6.7	130.1	5.3
Synaptobrevin-2	7	121	5.8
Syntaxin-1B	9	288	3.1
SNAP-25	14	206	6.8
Synaptotagmins 1–17	29.9	467.2	6.4
Complexins 1–4	11.3	146.5	7.7
Synaptophysin	39	313	12.5
Synapsins 1–3	50.3	622.3	7.9
β-synuclein	13	134	9.7
γ-synuclein	10	127	7.9

Advances in the atomic resolution of misfolded α-synuclein conformations

Several intrinsic and extrinsic factors influence the shape, pitch, twist, protofilament number, filament diameter, and inter- and intramolecular interactions to determine α-synuclein fibril morphology [42]. Reflective of these differences, a variety of conformations have been reported using multiple sources of recombinant α-synuclein, including wild-type (WT), mutant, post-translationally modified, and/or truncated protein (Table 2). In addition to differences in the starting protein monomer, fibrils have been generated using a variety of buffers and other experimental conditions, including pH and sonication (Table 3). In the

Table 2 Conserved structural elements in α-synuclein fibrils

PDB[a]	Length	Mutation	PTMs	Structural elements					
				Templating region	E46-K80 salt bridge	Interface	Cofactor	Kinetics[b]	Ref
2N0A	1–140	None	None	A29-K97	Present	Single protofilament	No	n.d.[c]	[100]
6XYP[d]	1–140	None	Ubiquitination, acetylation, phosphorylation	A: G14-F94 B: G36-Q99	A: Present B: Present	A: Q24-V55 B: L38-T64	Yes	n.d	[92]
6XYO[d]	1–140	None	Ubiquitination, acetylation, phosphorylation	A: G14-F94 B: K21-Q99	A: Present B: Present	A: Q24-E57 B: E35-T64	Yes	n.d	[92]
6XYQ[d]	1–140	None	Ubiquitination, acetylation, phosphorylation	A: G14-F94 B: G36-Q99	A: Present B: Present	A: Q24-V55 B: L38-T64	Yes	n.d	[92]
6CU8	1–140	None	None	K43-E83	Absent	V66-A78	No	n.d	[58]
6CU7	1–140	None	None	L38-K97	Present	H50-E57	No	n.d	[58]
6SST	1–140	None	None	G14-G25 & G36-K96	Absent	K45 and E46	No	n.d	[42]
6RTB	1–140	None	None	S9-Q24, E35-A56, & Q62-G93	Absent	K45 and E46	No	n.d	[42]
6SSX	1–140	None	None	G14-G25 & G36-K96	Absent	K45 and E57	No	n.d	[42]
6RT0	1–140	None	None	G14-G25 & G36-K97	Absent	K45 and E57	No	n.d	[42]
6L1T	1–140	None	Phosphorylation Tyr39	M1-L100	Absent	E57-K58	No	n.d	[114]
6L1U	1–140	None	Phosphorylation Tyr39	M1-L100	Absent	A & B: E57-K58 (both) B & C: E46 (B) and E57-K58 (C)	No	n.d	[114]
6A6B	1–140	None	N-terminal acetylation	V37-Q99	Present	H50-E57	No	n.d	[61]
6OSJ	1–140	None	N-terminal acetylation	V37-K97	Present	H50-E57	No	n.d	[76]
6OSL	1–122	None	N-terminal acetylation	Y39-K97	Present	H50-E57	No	n.d	[76]
6OSM	1–103	None	N-terminal acetylation	Y39-V95	Present	H50-E57	No	n.d	[76]
6H6B	1–121	None	C-terminal truncated (1–121)	L38-V95	Present	H50-E57	No	n.d	[43]
6FLT	1–121	None	C-terminal truncated (1–121)	L38-V95	Present	H50-E57	No	n.d	[43]
6UFR	1–140	E46K	None	G36-D98	Absent	K45-E57	Solvent filled	Increase	[12]
6L4S	1–140	E46K	N-terminal acetylation	K45-Q99	Absent	V74-Q79	No	Increase	[113]
6PES	1–140	H50Q	None	A: G36-Q99 B: T44-K97	A: Present B: Present	K58-E61	No	Increase	[11]
6PEO	1–140	H50Q	None	G36-Q99	Present	Single filament	No	Increase	[11]
7E0F	1–140	G51D	N-terminal acetylation	H50-D98	Absent	V74-Q79	No	Decrease	[97]
6LRQ	1–140	A53T	N-terminal acetylation	V37-Q99	Present	T59-K60	No	Increase	[96]

[a] *PDB* protein data bank ID number

[b] Relative to WT protein

[c] *n.d.* not determined

[d] Fibrils isolated from MSA patient samples contain two different protofibril structures (denoted A and B)

Table 3 α-synuclein fibril preparation conditions

PDB[a]	Protein concentration	Buffer conditions	pH	Temperature (°C)	Shaking & sonication conditions	Ref
2N0A	15 mg/mL	50 mM NaPi, 0.1 mM EDTA, 0.02% sodium azide (w/v)	7.4	37	200 rpm, 3 weeks	[100]
6CU8	300 µM	15 mM tetrabutylphosphonium bromide	Not specified	RT[b]	Not specified	[58]
6CU7	300 µM	15 mM tetrabutylphosphonium bromide	Not specified	RT	Not specified	[58]
6SST	700 µM	50 mM Tris HCl, 150 mM KCl	7.5	37	600 rpm (Eppendorf ThermoMixer), 1 week	[42]
6RTB	700 µM	50 mM Tris HCl, 150 mM KCl	7.5	37	600 rpm (Eppendorf ThermoMixer), 1 week	[42]
6SSX	700 µM	50 mM Tris HCl, 150 mM KCl	7.5	37	600 rpm (Eppendorf ThermoMixer), 1 week	[42]
6RT0	700 µM	50 mM Tris HCl, 150 mM KCl	7.5	37	600 rpm (Eppendorf ThermoMixer), 1 week	[42]
6L1T	100 µM	50 mM Tris 150 mM KCl, 0.05% NaN_3	7.5	37	900 rpm (Eppendorf ThermoMixer), 1 week; 30 s 20% power sonicated (1 s on/1 s off; JY92-IIN sonicator) on ice, mixed sonicated fibrils (0.5%, vol/vol) with monomer & repeated shaking incubation, 2 weeks	[114]
6L1U	100 µM	50 mM Tris, 150 mM KCl, 0.05% NaN_3	7.5	37	900 rpm (Eppendorf ThermoMixer), 1 week; 30 s 20% power sonicated (1 s on/1 s off; JY92-IIN sonicator) on ice, mixed sonicated fibrils (0.5%, vol/vol) with monomer & repeated shaking incubation, 2 weeks	[114]
6A6B	500 µM	50 mM Tris, 150 mM KCl, 0.05% NaN_3	7.5	37	900 rpm (Eppendorf ThermoMixer), 3 days; 30 s sonication of diluted 25 µM sample (1 s on/1 s off) on ice, mixed sonicated fibrils (0.5%, vol/vol) to 25 µM acetylated monomer & repeated shaking incubation, 3 days	[61]
6OSJ	100–300 µM	10 mM NaPi, 140 mM NaCl	7.4	37	600 rpm (VWR Mini-Micro 980,140 shaker), 4–5 days	[76]
6OSL	100–300 µM	10 mM NaPi, 140 mM NaCl	7.4	37	600 rpm (VWR Mini-Micro 980,140 shaker), 4–5 days	[76]
6OSM	100–300 µM	10 mM NaPi, 140 mM NaCl	7.4	37	600 rpm (VWR Mini-Micro 980,140 shaker), 4–5 days	[76]
6H6B	5 mg/mL	DPBS, Gibco; 2.66 mM KCl, 1.47 mM KH_2PO_4, 137.93 mM NaCl, 8.06 mM Na_2HPO_4-$7H_2O$	7.0–7.3	37	1000 rpm (Eppendorf orbital mixer), 5 days; 5 min sonication (Branson 2510 water bath)	[43]
6FLT	5 mg/mL	DPBS, Gibco; 2.66 mM KCl, 1.47 mM KH_2PO_4, 137.93 mM NaCl, 8.06 mM Na_2HPO_4-$7H_2O$	7.0–7.3	37	1000 rpm (Eppendorf orbital mixer), 5 days, 5 min sonication (Branson 2510 water bath)	[43]
6UFR	300 µM	15 mM tetrabutylphosphonium bromide	Not specified	37	Shaking speed not specified; 2 weeks	[12]

Table 3 (continued)

PDB[a]	Protein concentration	Buffer conditions	pH	Temperature (°C)	Shaking & sonication conditions	Ref
6L4S	100 µM	50 mM Tris, 150 mM KCl	7.5	37	900 rpm (Eppendorf ThermoMixer), 1 week; 20% power sonication × 15 (1 s on/1 s off; JY92-IIN sonicator) on ice, mixed sonicated fibrils (0.5 mol%) with 100 µM monomer & repeat shaking, 1 week	[113]
6PES	300 µM	15 mM tetrabutylphosphonium bromide	Not specified	37	Shaking speed not specified; 2 weeks	[11]
6PEO	300 µM	15 mM tetrabutylphosphonium bromide	Not specified	37	Shaking speed not specified; 2 weeks	[11]
7E0F	100 µM	50 mM Phosphate buffer, 50 mM NaCl, 0.05% NaN_3	7	37	900 rpm (Eppendorf ThermoMixer), 1 week; 20% power sonication × 15 (1 s on/1 s off; JY92-IIN sonicator) on ice, mixed sonicated fibrils (0.5 mol%) with 100 µM monomer & repeat shaking, 1 week	[97]
6LRQ	300 µM	D-PBS	Not specified	37	1000 rpm (Eppendorf ThermoMixer), 5 days; 20% power sonication × 22 (1 s on/1 s off) on ice, mixed sonicated fibrils (1% v/v) with 100 µM monomer & repeat shaking, 5 days	[96]

[a] *PDB* protein data bank ID number

[b] *RT* room temperature

following sections, we will discuss the effect that each of these factors has on protein structure. An important caveat to note, however, is that it remains unknown how similar mutations, post-translational modifications, or truncations impact the misfolded protein conformation in patients with synucleinopathies.

The first structural insights into α-synuclein misfolding came from Rodriguez et al. in 2015. Using micro-electron diffraction to resolve the structure of the 11-residue NACore segment of α-synuclein preformed fibrils (PFFs; residues 68–78), the authors reported that the short segments form steric zipper structures that are cytotoxic when incubated with cells [85]. However, there were two important questions about these structures following the initial publication. The first was if the 11-mer structure was consistent with the full-length α-synuclein fibrils found in synucleinopathy patients. And the second focused on how the known disease-causing *SNCA* mutations impacted protein misfolding. Insights into the latter question were first gained from the solid-state NMR (ssNMR) structure of full-length α-synuclein PFFs reported by Tuttle et al. in 2016 (Fig. 1c) [100]. In this structure, the templating region of α-synuclein, spanning residues 29–97, adopts a Greek key motif (four β-strands with + 3, − 1, − 1 topology [46]), which is flanked by a hydrophilic "fuzzy coat" created by the disordered N- and C-terminal residues of the protein. A salt bridge between residues E46 and K80 appears to be critical for stabilizing the Greek key in this structure. Intriguingly, a subset of familial LBD patients has a heterozygous E46K mutation in *SNCA*, suggesting that α-synuclein must adopt a distinct conformation from the one reported by Tuttle et al. in patients with the E46K mutation.

Recent advances in cryo-EM facilitated an explosion in the resolution of misfolded α-synuclein conformations (Fig. 2). With three exceptions, the cryo-EM structures of recombinant α-synuclein amyloids contain two symmetrical protofilaments that are stabilized by intramolecular electrostatic interactions [12, 42, 43, 58, 61, 76, 96, 97, 113, 114]. The outliers are (1) the recently reported trimer [114], (2) the single filament observed in the narrow H50Q fibril structure (Fig. 2c, inset), and (3) the asymmetrical H50Q wide fibril structure (Fig. 2c; [11]). In 2018, Li et al. resolved two general populations of full-length WT PFFs, termed the rod and twister polymorphs (Fig. 2a), which share a bent β-arch

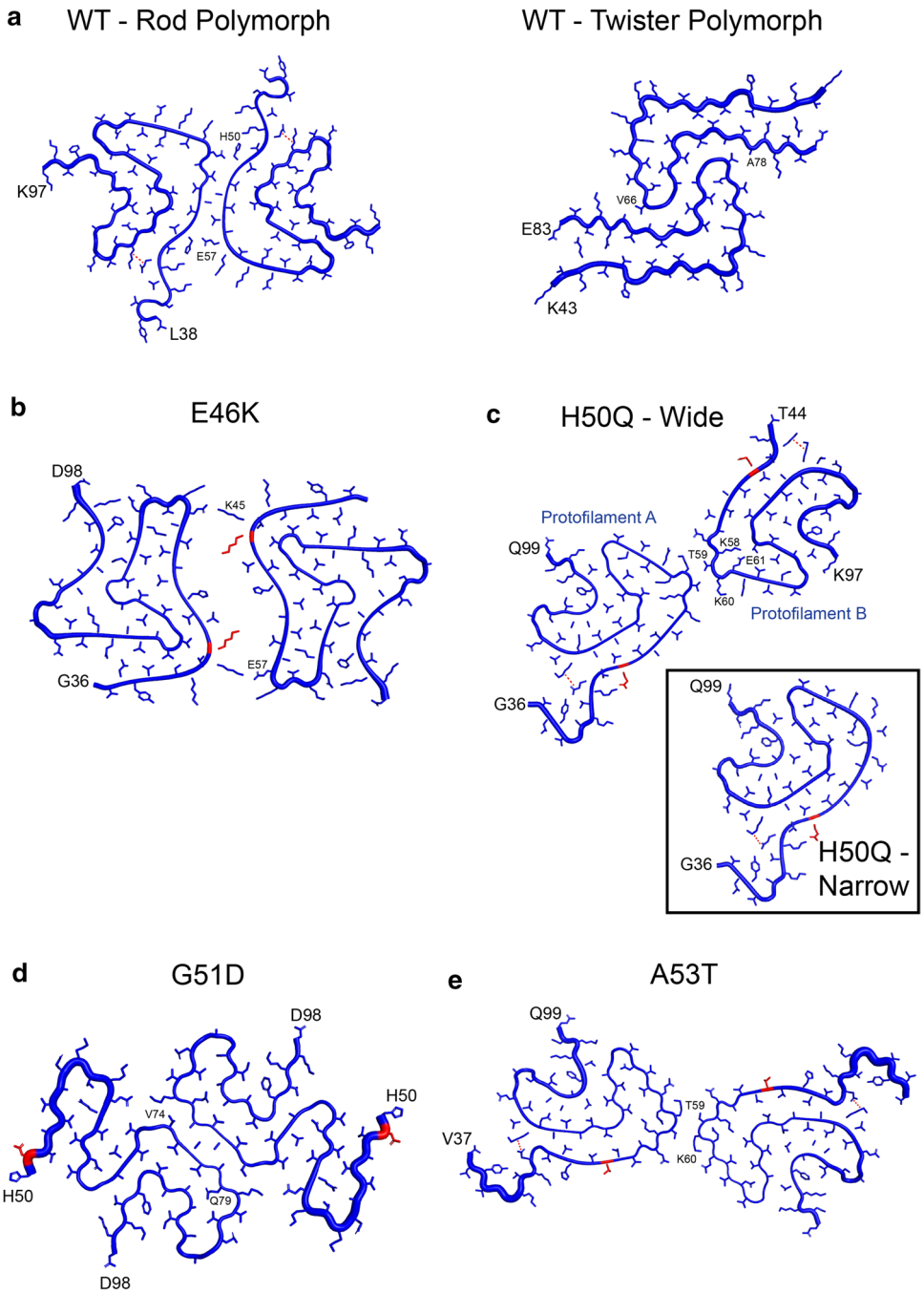

Fig. 2 Effect of familial Parkinson's disease mutations on α-synuclein fibril structure. Published structures of **a** WT or **b**–**e** mutant α-synuclein fibrils made from recombinant protein. Each of the Parkinson's disease-causing point mutations (E46K, H50Q, G51D, and A53T; mutant residue shown in red) alters the protofilament interaction seen in WT fibrils. **a** The rod polymorph WT structure (left) includes an inter-protofilament interface spanning residues H50-E57, which forms a tight hydrophobic interaction (PDB ID 6CU7, [58]). In contrast, the twister polymorph WT structure (right) includes an inter-protofilament interface comprised of residues V66-A78 (PDB ID 6CU8, [58]). **b** The E46K mutation results in a fibril structure that contains a solvent-filled interface that is stabilized by salt bridges between K45 and E57 on either end of the cavity (PDB ID 6UFR, [12]). **c** The H50Q mutation shifts the protofilament interface in the wide fibril structure to residues K58-E61 (PDB ID 6PES; [11]). H50Q wide fibrils contain two asymmetrical protofilaments, denoted Protofilament A and Protofilament B. The H50Q narrow fibril (inset) is a single protofilament with identical structure to Protofilament A (PDB ID 6PEO; [11]). **d** The G51D mutation shifts the protofilament interface and inhibits β-turn formation, leading to a serpentine structure unique from most other reported α-synuclein conformations (PDB ID 7E0F; [97]). **e** The A53T mutation results in a protofilament interface spanning residues T59-K60 (PDB ID 6LRQ, [96]). However, the overall filament structure is consistent with the folding seen in the **a** WT and **c** H50Q structures; a Greek key motif is stabilized by a salt bridge between residues E46 and K80 (dashed red line)

kernel structure (residues H50-V77) and a Greek key motif within each protofilament [58]. The major feature distinguishing these two structures is a varied protofibril interface. While the rod polymorph consists of an interface in the preNAC region (residues H50-E47), the twister polymorph interface occurs in the NACore (residues V66-A78). The preNAC region interface has subsequently been observed in several additional WT α-synuclein fibril structures, including acetylated and C-terminally truncated sequences [43, 58, 61, 76]. Here, the formation of a steric zipper at the protofibril interface is driven by hydrophobic interactions between nonpolar amino acids [43, 58, 61, 76].

Effect of mutations and other intrinsic factors on α-synuclein fibril structure

Amyloid strains are defined by unique biochemical and biophysical properties that manifest as distinct neuropathologies, clinical phenotypes, and incubation periods. The molecular dynamics and mechanisms governing α-synuclein misfolding into each specific conformation, or strain, remains unclear, but the presence of disease-causing mutations has been postulated to disrupt intra- and/or intermolecular interactions, placing constraints on the spectrum of misfolded conformations α-synuclein can adopt (Fig. 2). For example, the E46K mutation likely disrupts the E46/K80 salt bridge that stabilizes the Greek key motif, as discussed above, preventing α-synuclein misfolding into several of the reported amyloid structures. To date, nine mutations have been identified in familial LBD patients (A30G/P, E46K, H50Q, G51D, A53E/T/V, and T72M [3, 27, 29, 51, 55, 62, 67, 81, 111, 112]). Each of these mutations is reported to alter the fibrillization rate of α-synuclein, though it is unknown if this occurs by altering the misfolded protein conformation *or* by altering the energy barrier required for α-synuclein to adopt a particular conformation. Notably, it is also unclear if the reported effects on fibrillization kinetics alter the rate of α-synuclein prion formation, the rate of α-synuclein prion propagation, or both. However, altered aggregation kinetics alone are insufficient to determine if each mutation gives rise to a distinct strain. For some of the known familial *SNCA* mutations, cryo-EM has been used to resolve the structure of α-synuclein fibrils generated using recombinant mutant protein (Fig. 2), but the relevance of these structures compared to the fibrils found in patients harboring the same mutation is not known. Moreover, the lack of animal and cellular data pertaining to the biological properties associated with each mutation limits our ability to determine the effect of each *SNCA* mutation on α-synuclein strain behavior. In the following sections, we will discuss the impact of the nine known mutations on α-synuclein structure and kinetics based on studies using recombinant fibrils. However, this discussion requires the critical caveat that due to a lack of standardized α-synuclein strain biology assays and cryo-EM structures from LBD patients, these conclusions may not be an accurate representation of the effect of each mutation on α-synuclein strain biology in LBDs. Moreover, while mutant α-synuclein is often used to investigate disease pathogenesis in LBDs, it is important to note that around 15% of PD cases are inherited, while *SNCA* mutations are estimated to account for only ~ 2% of cases [6, 56, 99]. Further, because familial PD cases are infrequent worldwide and many patients are never subject to genetic testing, the frequency of each α-synuclein mutation is difficult to establish. As a result of the rarity in *SNCA* mutations, we will structure our discussion by contrasting the effect of each mutation on α-synuclein structure with structures reported using WT α-synuclein fibrils.

A30G/P

While the A30P mutation was reported in 2001 [50], the A30G mutation was recently described in three families with typical parkinsonian symptoms in early 2021 [62]. The A30P and A30G mutations have each been identified in 3 and 5 confirmed PD cases, respectively [62, 86]. Patients with the A30G/P mutations have a variable age of onset, ranging from 54–76 to 36–80 years of age, respectively, and present with resting tremor, rigidity, or bradykinesia. Interestingly, A30G patients are more likely to develop non-motor symptoms, including orthostatic hypotension, urinary incontinence, and rapid eye movement behavioral disorder, as well as psychiatric symptoms, including hallucinations, depression, and cognitive decline. Structurally, both mutations decrease the α-helical propensity of soluble α-synuclein [62], but exert differing effects on fibrillization. The replacement of an alanine with a glycine increases protein flexibility, resulting in fibrillization kinetics that are similar to or faster than WT α-synuclein when monitored by thioflavin T (ThT) incorporation. Alternatively, the proline substitution inserts a kink or bend in the amino acid sequence, significantly decreasing the rate of fibrillization [62, 110]. Macroscopically, A30P fibrils are more densely packed than WT α-synuclein [77], suggesting the fibrils may be more resistant to fragmentation, which would decrease the efficiency of additional templating and fibrillization. The exact effect of the A30G/P mutations on α-synuclein structure are unknown as there are currently no published structures containing these mutations. Notably, the location of these two mutations outside of the preNAC region makes them unique with regard to the majority of LBD mutations. While many of the other mutations disrupt the reported protofilament interfaces, A30 is often located outside of the templating region in α-synuclein amyloids, suggesting the effect it has on fibril structure is distinct from the effects of other known mutations.

E46K

The E46K mutation is the second-most common *SNCA* mutation, associated with 10 confirmed cases of PD. Patients harboring this mutation typically have an age of onset between 50 and 65 years of age and present with severe parkinsonian symptoms and dementia [86, 112]. In addition, some patients also progress to experience visual hallucinations. The first reported structure containing the E46K mutation was resolved from mutant PFFs by Boyer et al. in 2020 (Fig. 2b) [12]. In this structure, residues K45-E57 form a solvent-filled protofilament interface that is stabilized by two electrostatic interactions between residues K45 and E57 on each end of the interface between the protofilaments, respectively. A positively charged lysine and histidine residue from each of the two protofilaments projects into the resulting cleft, which contrasts with the highly hydrophobic H50-E57 interface commonly observed in WT α-synuclein structures (Figs. 2a, b; [42, 58, 61, 76]). Using N-terminally acetylated E46K PFFs, Zhao et al. reported a structure containing a hydrophobic protofilament interface between residues V74-Q79 (Fig. 3) [113]. The shifted interface increases the flexibility of the N-terminal region of the fibril core, likely contributing to a looser fibril packing, which resulted in a lower fibril stability when compared to WT fibrils [113]. This reduced stability may lead to an increase in fibril fragmentation, contributing to the observed increase in aggregation rate in ThT assays [113]. While the E46K structures reported by Boyer et al. and Zhao et al. exhibit structural differences, both fibrils maintain either an increased rate of aggregation or an enhanced cytotoxicity, respectively, when compared to WT PFFs. However, more data are needed to determine if these changes are the direct result of the mutation or if they are due to differences in experimental conditions.

Notably, aside from the A53V mutation [111], familial *SNCA* patients are heterozygous for mutations, meaning that mutant protein is co-expressed with WT α-synuclein. Investigating the ability of E46K PFFs to template using WT recombinant protein and vice versa, Long et al. reported that WT α-synuclein adopts the E46K conformation when seeded with E46K PFFs, despite the mismatch in the amino acid sequence [64]. However, WT fibrils could not cross-seed E46K monomer, likely due to disruption of the salt bridge formed between residues E46 and K80 in the WT fibril structure [61, 92, 100]. The change from a glutamic acid to a lysine causes a charge–charge repulsion with K80, destabilizing the β-arch observed in most α-synuclein structures, resulting in what is likely unidirectional cross-seeding between WT and E46K α-synuclein. These findings are consistent with transgenic mouse studies showing that WT PFFs (containing residues 21–140) injected into the hippocampus

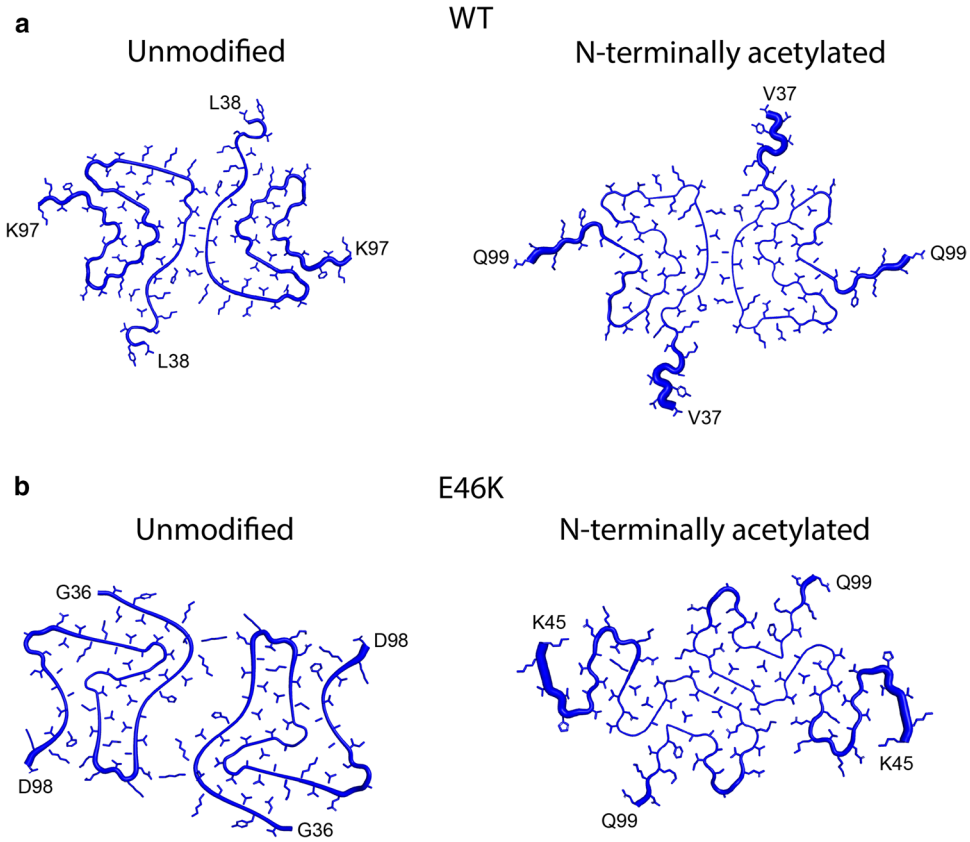

Fig. 3 Effect of acetylation on α-synuclein fibril structure. N-terminal acetylation appears to have little effect on **a** WT α-synuclein fibril structure, but **b** substantially impacts E46K fibrils. **a** Unmodified WT α-synuclein (left; PDB ID 6CU7, [58]) and N-terminally acetylated α-synuclein (right; PDB ID 6A6B, [61]) maintain the same H50-E57 protofilament interface, along with similarities in the β-folds. **b** In contrast, E46K fibril structure differs substantially when N-terminally acetylated E46K protein is used to generate fibrils (unmodified on left, PDB ID 6UFR, [12]; acetylated on right PDB ID 6L4S, [113])

of TgM47 mice, which express human E46K α-synuclein, induce minimal α-synuclein pathology 4 months post injection [89].

H50Q

The H50Q mutation is rare (3 confirmed cases), and results in a clinical presentation of tremor followed by motor decline, speech problems, and cognitive impairment around 60 years of age [3, 82, 86]. Boyer et al. reported two H50Q polymorphs: a narrow fibril containing one protofilament and a wide fibril containing two asymmetrical protofilaments. In the wide fibril (Fig. 2c), protofilament A contains a longer templating region than protofilament B with residues K45 and Q50 slightly differing in orientation [11]. Overall, each protofilament is similar to the WT fibril conformations, but the H50Q fibrils have a shorter steric zipper protofilament interface (residues K58–E61 versus H50-E57 in the WT fibrils) involving residues outside of the preNAC (residues H/Q50-E57) and NACore (residues V66-A78) regions [11, 58]. In several WT α-synuclein fibril structures, residue H50 forms a salt bridge with either residue E57 or E58, which stabilizes the hydrophobic steric zipper. The presence of the H50Q mutation disrupts this interaction, which destabilizes the hydrophobic interface discussed above [58] and shifts the residues involved in intramolecular bonding at the protofilament interface [11]. As a result, residues H50-E57 form a straight β-strand segment with minimal inter-filament interactions in the wide H50Q fibril. Moreover, Q50 can now form an electrostatic interaction with K45 on the same strand, creating a slight bend in the fibril [11]. The conformation is also stabilized by an internal salt bridge between K58 and E61. Cell-free fibrillization assays using H50Q α-synuclein indicate that the mutation results in faster fibrillization kinetics compared to the WT protein [11, 88]. In addition, compared to sonicated WT PFFs, sonicated H50Q PFFs induced more protein aggregation in α-syn140*A53T-YFP cells, as well as more cytotoxicity in differentiated PC12 cells as measured by MTT assay [11]. However, it is unclear if these findings are due to differences in protein conformation or a difference in the number of free ends available for self-templating following sonication.

G51D

The G51D mutation has been identified in 8 cases of PD [86]. Patients with the G51D mutation have a unique presentation with an early age of onset (typically in their 30 s) and a rapidly progressive phenotype with only a few years between patient diagnosis and death [48, 55]. Affected patients exhibit typical parkinsonism that quickly progresses, resulting in loss of autonomy, as well as psychiatric symptoms including anxiety and hallucinations. The G51D mutation substitutes a larger hydrophilic residue for the normal hydrogen, which would disrupt the hydrophobic protofilament interface. Sun et al. recently reported a structure of N-terminal acetylated G51D α-synuclein and discovered an extended serpentine fold that is unique from previously determined fibril structures (Fig. 2d) [97]. This mutation results in the formation of a β-hairpin that shifts the protofilament interface to residues V74-Q79 (H50-E57 in WT) [97]. Like E46K fibrils, G51D fibrils exhibit a right-handed helical twist. However, while the K45-E57 salt bridge is enabled by a β-turn that includes residue G51 in the E46K fibrils, the G51D mutation inhibits the β-turn from forming, leaving the N-terminal portion of the fibril flexible [97]. As a result, G51D α-synuclein cannot adopt either the WT or E46K structures (Fig. 2). However, G51D fibrils are capable of cross-seeding WT α-synuclein (WT_{51cs}) [97]. This finding, in combination with the E46K cross-seeding studies, suggests that WT α-synuclein can misfold into a large number of possible conformations, but the presence of specific mutations, such as E46K and G51D, constrains protein misfolding to a subset of the total possible conformations.

Biochemical studies have shown that recombinant G51D α-synuclein exhibits a decreased association with phospholipid membranes and slower fibrillization kinetics compared to WT protein [27, 88, 97]. Consistent with this observation, when Sun et al. compared the effect of sonication on WT versus G51D fibrils, they observed that the G51D fibrils fragmented into smaller species. However, when the sonicated fibrils were incubated with primary neuronal cultures, the G51D PFFs induced more α-synuclein aggregation than the WT fibrils [97]. These cellular data are difficult to interpret given that fibril fragmentation via sonication increases the number of free ends available for templating. As a result, the differences in aggregate formation may be a reflection of the number of exposed surfaces available to catalyze α-synuclein misfolding rather than differences in misfolding kinetics.

A53E/T/V

While there are three known point mutations at residue A53, the A53T mutation is the most commonly reported of all *SNCA* mutations, having been identified in ~ 150 cases around the world [86]. Of the reported A53T cases, about half have been genetically confirmed while the others are genetically unconfirmed familial cases [86]. The A53E and A53V mutations have been linked to 7 and 2 cases of Parkinson's disease, respectively [86, 111]. In addition to differences in mutation prevalence, the reported onset of clinical disease also differs between the three mutations. The earliest reported age of onset is in patients with the A53E mutation (~ 34 years old), followed by A53T (~ 47 years old) and then A53V (~ 56 years old) [67, 80,

81, 111]. These mutations also result in varied clinical presentations. A53E patients exhibit severe bradykinesia but no cognitive decline whereas A53T patients develop autonomic dysfunction and dementia. These are both in contrast to A53V patients who typically suffer from tremors, hallucinations, and cognitive decline, similar to the presentation of DLB [49, 69]. A53 is in the center of the protofilament interface in WT α-synuclein PFFs, meaning mutations to this residue are likely to disrupt or shift the intermolecular interactions between the fibril strands. Consistent with this hypothesis, Sun et al. reported a cryo-EM structure of A53T α-synuclein PFFs showing that the neutral threonine disrupts the hydrophobic zipper, resulting in a shorter protofilament interface (residues T59-K60) that makes the fibril less stable (Fig. 2e) [96]. This is compounded by the loss of the H50/E57 salt bridge between the two filaments. Biochemically, A53T fibrils exhibit an enhanced fragmentation rate, increased aggregation propensity (measured by ThT incorporation), and greater cytotoxicity in SH-SY5Y cells compared to WT α-synuclein, which may be due to the observed decrease in structural stability between the WT and mutant conformations [73, 74, 96]. In contrast, the A53E mutation reduces α-synuclein fibrillization compared to WT, resulting in the formation of oligomeric protofibrils, instead [35, 54, 87]. While the mechanism by which this mutation leads to disease remains unclear, the mutation has been shown to cause a number of cellular pathologies, including fragmentation of the Golgi body. Finally, Mohite et al. reported that A53V fibrils exhibit decreased membrane interactions and enhanced aggregation kinetics relative to WT protein [73]. While there are currently no cryo-EM structures of the A53E or A53V mutations available, the notable structural differences between WT and A53T fibrils (Fig. 2) suggest that it may be difficult to translate discoveries made using A53X model systems to WT α-synuclein.

T72M

Most recently, the T72M point mutation was discovered in two Turkish families [29]. These patients presented with variability in the occurrence of non-motor clinical features and an age of onset ranging from 39 to 57 years, but both families displayed cognitive decline [29]. Disease onset is consistent with what is observed in patients harboring the A53E and G51D mutations, however, these mutations lie within the preNAC region while T72M is in the NACore domain. While it is unclear how the substitution of a small hydrophilic amino acid for a large hydrophobic residue impacts protein misfolding, fibrillization studies using ThT incorporation showed that T72M α-synuclein exhibits accelerated aggregation kinetics compared to WT protein [29].

Effect of post-translational modifications on α-synuclein structure

In addition to the mutations discussed above, α-synuclein can undergo several post-translational modifications (PTMs), including phosphorylation, acetylation, nitration, ubiquitination, O-GlcNAcylation, and truncation [2, 57]. It is currently unclear what specific role PTMs play in disease pathogenesis, or even when the modifications occur (i.e., before or after fibril formation). As a result, it is difficult to parse out how each PTM may contribute to the varied clinical presentations seen across synucleinopathy patients. Efforts to understand the effect of PTMs on α-synuclein strain formation include the use of cryo-EM to determine structural differences between fibrils formed using WT versus modified recombinant protein. For example, phosphorylation of Y39, which has been observed in PD patients [15], results in either a twisted dimer or trimer structure, both of which contain the largest reported core region for any α-synuclein fibril, spanning residues 1–100 [114]. Importantly, α-synuclein is N-terminally acetylated under physiological conditions [2]. However, N-terminal acetylation of full-length α-synuclein has varying effects on fibril structure that appear to be dependent upon whether the PTM is present on WT or mutant α-synuclein, or if other PTMs are present. Cryo-EM studies suggest the structure of WT α-synuclein is largely unaltered by the presence of N-terminal acetylation, which is likely due to the location of the acetyl group outside of the observed templating region (Fig. 3a) [76]. In contrast to WT α-synuclein, N-terminal acetylation is associated with multiple changes to the E46K α-synuclein structure, including a shorter templating region and a shift in the protofilament interface of the fibrils (Fig. 3b). Consequently, the structures derived from un-acetylated mutant α-synuclein may be less likely to exist in human patients carrying the same mutation. While the location of the PTM may contribute to the varied impacts on α-synuclein structure reported to date, it is also possible that the conformations are dependent upon small differences in the fibrilization conditions (discussed below). As a result, we cannot untangle the effects of PTM and fibrillization conditions on fibril structure at this time. However, it is clear that additional studies are needed to fully determine how PTMs influence α-synuclein structure.

Effect of fibrillization environment on strain formation

Protein tertiary structure is dependent upon a variety of factors, including pH, temperature, and solvent. Recombinant α-synuclein is typically fibrillized at physiological temperature (37 °C) and pH (~ 7.5), but a variety of buffer conditions are used to generate the fibril structures

discussed above (Table 3). Given the large number of variables that can be altered under each experimental condition [41, 70, 71, 90], it is difficult to determine the exact effect of each variable on α-synuclein fibril formation. However, recent work by Lau et al. provides critical insight into the effect buffer conditions have on α-synuclein strain formation [53]. Recombinant PFFs generated in buffer containing either salt (S) or no salt (NS) yielded two distinct fibril species, each with unique biochemical properties. Inoculation studies comparing transmission of the two fibrils to the TgM83$^{+/-}$ mouse model, which expresses human α-synuclein with the A53T mutation [36], resulted in distinct incubation periods, clinical presentations, and pathological lesion profiles in the brain. Moreover, these properties were maintained upon serial passaging in the mice, consistent with the prion strain hypothesis. These findings suggest that future studies investigating the effect of specific salts or metals in fibrillization buffers may shed important light on key factors in the cellular environment that impact α-synuclein strain formation.

Redefining a strain

Due to a lack of structural data, prion strains have historically been defined operationally as isolates that consistently transmit neurological disease to a host, faithfully maintaining specific characteristics while doing so (i.e., incubation period, neuropathological lesion profile, biochemical stability, etc. [8]). However, recent advances in cryo-EM have enabled structural biologists to resolve the misfolded protein structures responsible for prion diseases. This renaissance offers the field a unique opportunity to redefine strains based on both protein structure and the resulting biological consequences in a host. An important question to address through this work is what degree of structural variability is required to induce distinct disease phenotypes. As discussed above, mutations, PTMs, and fibrillization environment all impact protein misfolding, however, there are multiple conserved structural elements across the reported α-synuclein structures (Table 2, Fig. 4). For example, α-synuclein PFF structures containing the H50Q and A53T mutations contain one identical protofilament (Fig. 4a), though they have differing fibril interfaces that result in a slightly skewed orientation of the second protofilament (Figs. 2c, e). The overlap in clinical

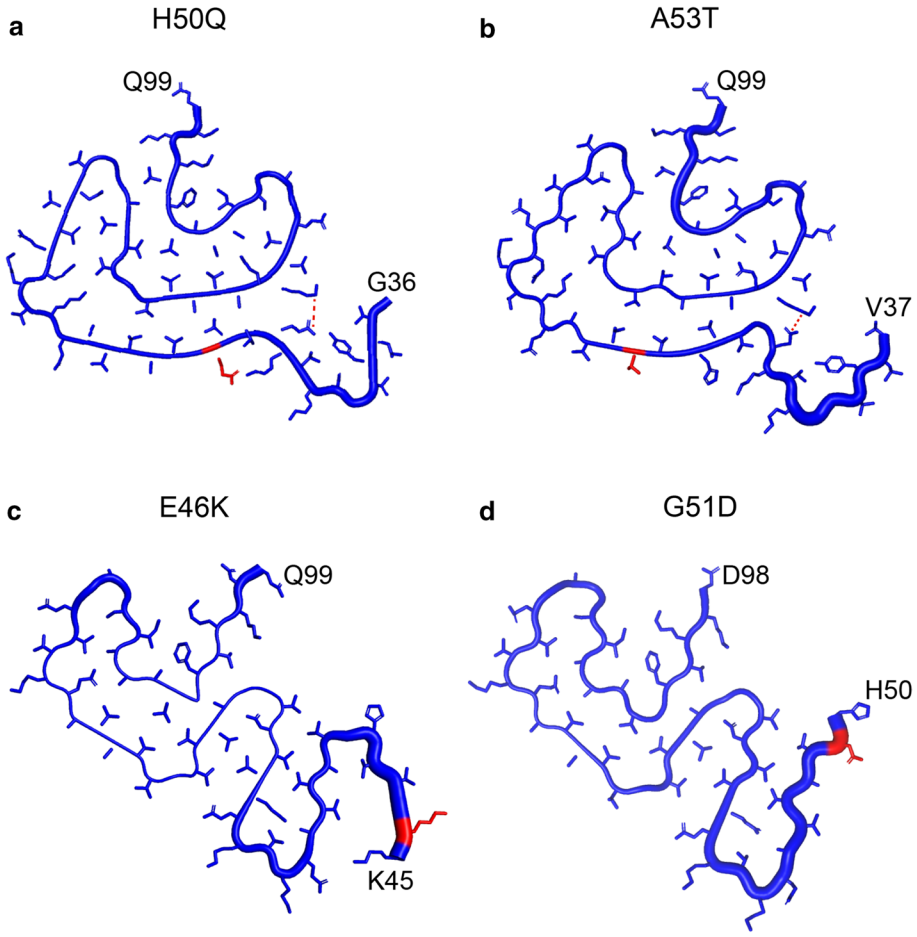

Fig. 4 Point mutations contribute to structural variability in the misfolded α-synuclein conformation. Comparison of single protofilaments from H50Q, A53T, E46K, and G51D recombinant α-synuclein fibril structures shows structural similarity between the **a** H50Q (PDB ID 6PES, [11]) and A53T fibrils (PDB ID 6LRQ, [96]). The E46/K80 salt bridge is shown via dotted red lines. These conformations are distinct from the **b** N-terminally acetylated E46K (PDB ID 6L4S, [113]) and G51D fibril structures (PDB ID 7E0F, [97]). Mutated residues are highlighted in red

presentation in patients with the two mutations raises the possibility that the observed structural homology may converge on a particular set of disease characteristics. In comparison, E46K fibrils have a drastically different protein conformation from H50Q and A53T fibrils, consistent with the varied clinical presentation seen in patients with the E46K mutation (Fig. 2). Similarly, the serpentine structures from N-terminally acetylated E46K and G51D fibrils share several features, including protofilament interface (V74-Q79; Fig. 4b). As a result of the disrupted E46/K80 salt bridge, the E46K and G51D structures exhibit a shift in protofilament interface compared to the H50Q and A53T fibril structures. However, despite these similarities, the G51D mutation inhibits the formation of the β-turn seen in the E46K fibril structure. All together, these structures highlight a gap in understanding how many distinct α-synuclein strains exist and what degree of structural variation is required for two conformations to give rise to unique clinical phenotypes. For example, it is possible that the conservation of key criteria across structures results in similar clinical phenotypes. However, a major caveat to this interpretation is that it is unknown if any of these structural features are present in α-synuclein fibrils isolated from PD patients with or without *SNCA* mutations. Without a PD patient-derived structure of α-synuclein, the ability of the reported cryo-EM conformations to accurately model or predict α-synuclein strain biology in LBD patients remains unknown.

Structural differences between patient-derived fibrils and PFFs

In 2020, Schweighauser et al. reported the first patient-derived α-synuclein fibril structures from MSA patient samples [92]. Unlike the symmetry found in most reported PFF structures, this work identified two different asymmetrical filaments with a more extensive fibril interface, differentiated as Type I and Type II fibrils (Fig. 5). Both structures consist of two distinct protofilaments around a cavity containing a non-proteinaceous, negatively charged molecule, with the positively charged K43, K45, and H50 residues stabilizing the interaction [92]. Notably, while a non-protein density is observed in a handful of PFF structures [42, 43], it is unclear if it is the same cofactor that is present in the central cavity of the MSA structures. Additionally, MSA protofilaments adopt extended folds within the N-terminal region that are not observed in many of the PFF structures (see Templating Region in Table 2). Altogether, the structural differences between fibrils isolated from patient samples versus generated using recombinant protein add to growing concerns about the ability of PFFs to successfully replicate α-synuclein strain biology in human disease.

In an attempt to generate PFFs that replicate the α-synuclein structures in human patient samples, Shahnawaz et al. used real-time quaking induced conversion (RT-QuIC) to amplify α-synuclein oligomers from the cerebrospinal fluid of MSA and PD patients [93]. The kinetics of misfolding differed between the two sets of samples, and analysis by cryo-electron tomography and circular dichroism indicated that the structural differences in the resulting α-synuclein fibrils could be used to differentiate PD from MSA patient samples [93]. However, in 2021, Lövestam et al. used the same amplification methods to generate MSA-derived PFFs and resolved the fibril structures via cryo-EM [65]. These reactions yielded multiple filament structures that differed from the original MSA samples in several ways, including the absence of a non-protein density between two symmetrical protofilaments with altered protofibril interfaces [65]. Additionally, others have used protein misfolding cyclic amplification (PMCA) to amplify misfolded α-synuclein from PD- and MSA patient brain extracts and found that the in vitro generated α-synuclein structures were more similar to reported PFFs than to the reported brain-derived patient structures [33, 95]. These findings indicate that the published reaction conditions for RT-QuIC and PMCA cannot be used to faithfully propagate the α-synuclein structures in MSA.

Clinical consequences of α-synuclein structural heterogeneity

While recent advances in cryo-EM have revolutionized our ability to understand misfolded protein structure, it is important to recognize that these datasets represent a fixed time point in the disease process and are limited in what they can teach the field about the process of protein misfolding. For example, to understand the effect of *SNCA* point mutations on fibril structure, mutant protein alone is typically used to form PFFs. However, as noted above, patients are usually heterozygous for these mutations, meaning they express both WT and mutant α-synuclein. By forming PFFs in the absence of both WT and mutant protein, there are a number of questions left unanswered about how the presence of WT protein impacts the kinetics of mutant α-synuclein misfolding, or even if WT α-synuclein is incorporated into the pathogenic fibrils found in LBs. Additionally, there is often little biochemical or biological data reported along with a misfolded α-synuclein structure. Currently, the only complete dataset available for an α-synuclein strain, including fibril structure, biochemical properties, biological activity in cells and mice, etc., is for MSA (Fig. 6) [53, 83, 92, 105, 107, 108]. The lack of in vitro and in vivo correlations with PFF structures impedes our ability to draw conclusions

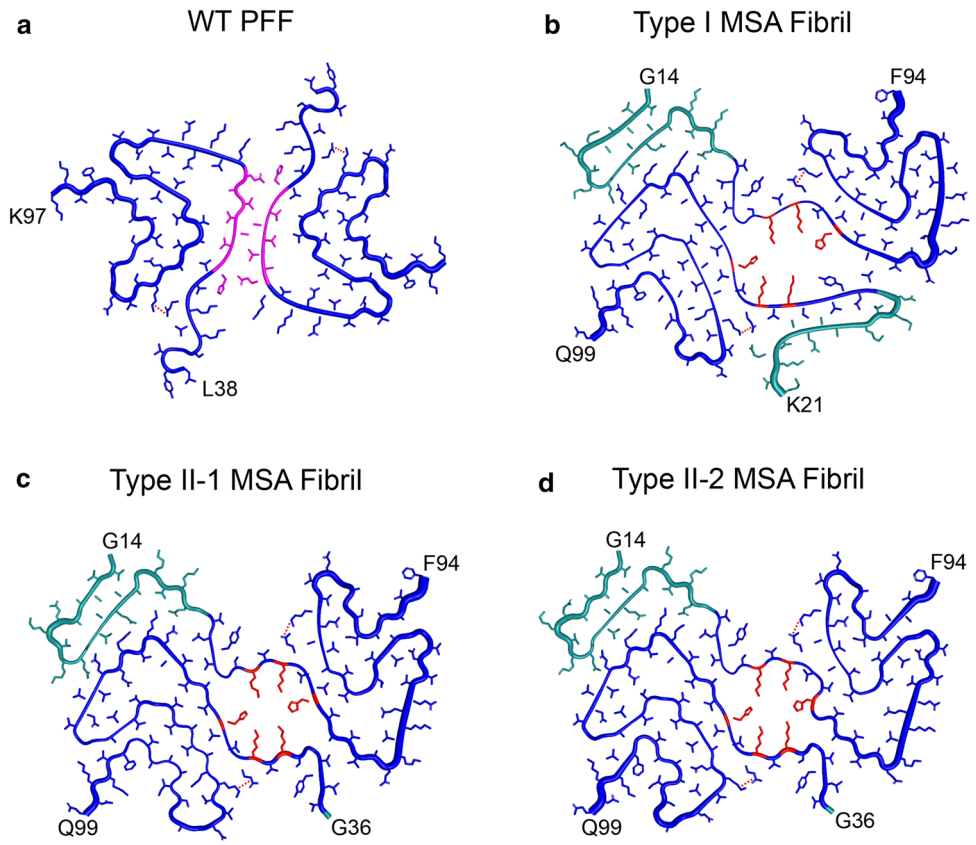

Fig. 5 A-synuclein fibrils isolated from multiple system atrophy patient samples are structurally distinct from recombinant fibril structures. **a** The templating region in wild-type (WT) α-synuclein fibrils spans residues 38–97 (PDB ID 6CU7, [58]). Two symmetrical protofilaments form a fibril interface between residues 50–57 (pink). **b**–**d** A-synuclein fibrils isolated from multiple system atrophy (MSA) patient samples contain two asymmetrical protofilaments with charged residues (red) at the protofibril interface, which interact with a non-proteinaceous molecule [92]. The asymmetrical protofilaments contain one filament with a longer templating region (residues 14–94) and one with a shorter templating region [either residues **b** 21–99 or (**c**, **d**) 36–99]. The N terminus of the MSA fibrils (light blue) adopts an extended fold that is not present in the **a** WT structure. PDB IDs for MSA fibrils: **b** 6XYO; **c** 6XYP; **d** 6XYQ, all reported in [92]. Salt bridge between E46 and K80 shown via dashed red lines

about the biological and clinical consequences of variation in fibril structure.

Notably, the methods used to determine misfolded protein conformations are unable to capture the diversity of structures that exist in a sample. Class averaging is used to improve the signal-to-noise ratio in the images that are collected by cryo-EM, and individual images are classified based on similarities in viewing direction, register, and rotational orientation [44, 91]. This classification provides an average that can then be used to create a final reconstructed 3D tomographic image. As a result, using class averaging to reconstruct a single α-synuclein structure may lead to an oversimplification of disease by selecting for a dominant protein conformation while also disregarding the presence of PTMs. A growing body of research in the prion field indicates that prion strains are made up of a spectrum, or "cloud," of many conformations that may evolve throughout the self-templating process, with one conformation emerging as the predominant structure in disease [20, 59]. This is seen in viral quasi-species, where a population of viruses with an array of genetic mutant spectra can increase or decrease in frequency during the replication process [23–25]. It is, therefore, critical to understand the clinical implications of the cloud hypothesis for studying and treating disease.

As new model systems and assays are developed to study α-synuclein strain biology, investigators need to consider how the conformational cloud may adapt within the model system(s) they are using. Introducing the cloud to a new host, as is done in animal and cellular bioassays, in addition to in vitro conversion assays, may select for one or two conformations within the cloud of α-synuclein structures that form a strain, as shown in Fig. 7. This complicates therapeutic development for several reasons. First, the factors responsible for in vivo strain maintenance are not yet known, and if the target assay fails to incorporate all components necessary, changes in the selective pressure of the host

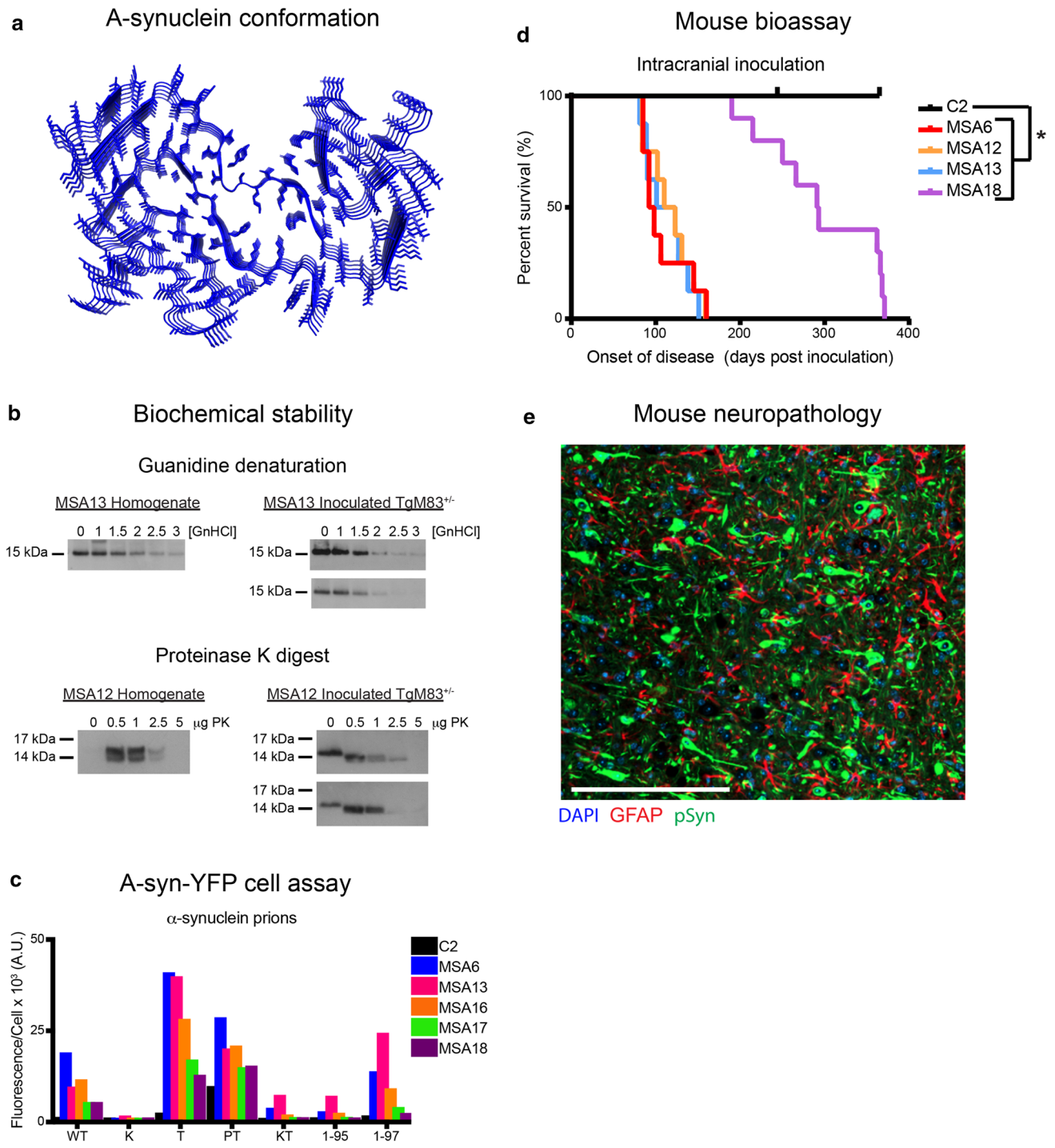

Fig. 6 Structural, biochemical, and biological criteria for defining the multiple system atrophy α-synuclein strain. Currently, no standardized criteria exist for defining individual α-synuclein strains across research laboratories. To better support synucleinopathy research across groups, we propose using a standard set of assays to define strains, including **a** structure, **b** biochemistry, **c** in vitro propagation using an array of substrates, **d** animal bioassay, and **e** neuropathological inclusions. **a** MSA TypeII-1 fibril structure (PDB ID 6XYP, [92]). **b** Degradation profiles for MSA α-synuclein from patient samples (left) or mouse-passaged patient samples (right) following guanidine denaturation (top) and proteinase K digestion (bottom). Primary antibody, EP1536Y. (Data published in [106].) **c** MSA propagation in HEK293T cells expressing various α-synuclein-YFP substrates (data published in [108]). WT, wild-type; K, E46K; T, A53T; PT, A30P and A53T; KT, E46K and A53T; 1–95, α-synuclein truncated at residue 95 with the A53T mutation; 1–97, α-synuclein truncated at residue 97 with the A53T mutation. **d** Kaplan–Meier plot from TgM83$^{+/-}$ mice inoculated with either control or MSA patient samples (data published in [107]). **e** A-synuclein neuropathology in a terminal TgM83$^{+/-}$ mouse inoculated with an MSA patient sample. Phosphorylated α-synuclein (pSyn; green), glial fibrillary acidic protein (GFAP; red), and nuclei (DAPI; blue). Scale bar, 200 microns. Data published in [107]

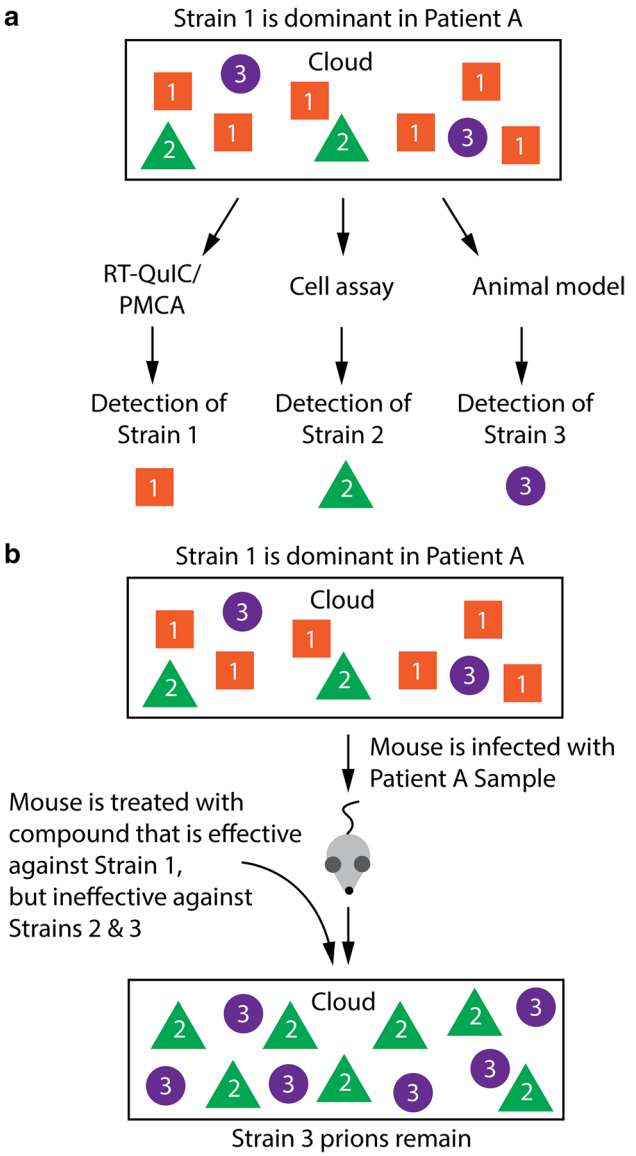

Fig. 7 Consequences of the cloud hypothesis for studying and treating α-synuclein strains. The cloud hypothesis posits that a strain is made up of a mixture of misfolded protein conformations, with one particular conformation emerging as the dominant structure in the strain. **a** A single patient sample (hypothetical Patient A) may contain multiple conformations, shown as strain 1 (orange squares), strain 2 (green triangles), and strain 3 (purple circles), but one of these conformations, strain 1, emerges as the predominant conformation in disease. However, when the environmental conditions that contributed to strain formation and maintenance are altered, for example, the patient sample is tested in an array of cell-free, in vitro, and in vivo assays, adaptation occurs and other sub-strains emerge as the dominant strain. **b** Under these conditions, high throughput screening of small molecules in a cell-free or in vitro assay will result in the identification of compounds that are ineffective in an in vivo model of disease. For example, when mice are inoculated with brain homogenate prepared from Patient A samples, a compound for strain 1 will suppress strain 1 propagation, but that will also contribute to the emergence of strains 2 and 3 in the mice. Under these conditions, the animals will still develop disease

will result in the emergence of a different dominant strain. Moreover, these changes may be assay-dependent, meaning that one structure will emerge in a cell-free or cellular assay and a different structure from the same conformational cloud will emerge in a mouse model (Fig. 7a). As a result, strain adaptation will impact the ability of a screening assay to predict in vivo compound efficacy, as well as the translatability of a compound from animal studies into the clinic. Second, changes in selective pressures on a cloud of conformations can result in drug resistance. A therapeutic that blocks the conversion of the dominant strain in a mixture can allow minor conformations to emerge, which will eventually cause clinical disease (Fig. 7b). This phenomenon has been observed in PrP prion diseases. Treatment with either swainsonine or the 2-aminothiazole, IND24 (discussed more below), resulted in the emergence of drug-resistant PrP^{Sc} strains, both of which reverted to a susceptible phenotype after drug removal [9, 59, 60].

Finally, redefining strains based on the protein conformation(s) that give rise to a specific disease phenotype is needed to successfully develop strain-specific therapeutics for synucleinopathy patients. The ramifications of prion strain variability previously thwarted efforts to develop therapeutics to halt PrP^{Sc} propagation in patients with Creutzfeldt–Jakob disease (CJD). A cell model that propagates the mouse-adapted scrapie PrP prion strain RML (isolated at Rocky Mountain Laboratories) was used to screen for small molecule inhibitors of PrP^{Sc} propagation [66]. This screen resulted in the identification of IND24, which doubles the lifespan of mice inoculated with RML prions. However, when IND24 was used to treat mice inoculated with CJD prions, the compound had no effect on survival [9, 34], underscoring the importance of incorporating strain-specificity in therapeutic development.

Conclusion

The widespread use of PFFs in synucleinopathy research has allowed investigators to interrogate the effect of *SNCA* mutations on α-synuclein structure and aggregation kinetics. However, the dearth of studies correlating in vitro and in vivo assays with protein structures limits our ability to draw connections between α-synuclein conformations and disease phenotypes. The need to establish this link is underscored by the conformational differences between PFFs and patient-derived fibrils; it remains unclear how predictive PFFs are of the α-synuclein biology that contributes to human disease. It is, therefore, imperative that structural studies be combined with a robust biological characterization to determine which reported structural components are clinically relevant.

Acknowledgements The Woerman Lab is supported by a Venture Grant (668-2020-06) from the CurePSP Foundation and the University of Massachusetts Amherst (A.L.W.). We thank Dr. Steven H. Olson for his thoughtful feedback on and intellectual discussions about the manuscript.

Declarations

Conflict of interest A.L.W. is a member of *Acta Neuropathologica*'s Editorial Board. They were not involved in the assessment or decision-making process for this manuscript.

References

1. Allison JR, Varnai P, Dobson CM, Vendruscolo M (2009) Determination of the free energy landscape of alpha-synuclein using spin label nuclear magnetic resonance measurements. J Am Chem Soc 131(51):18314–18326
2. Anderson JP, Walker DE, Goldstein JM, de Laat R, Banducci K, Caccavello RJ et al (2006) Phosphorylation of Ser-129 is the dominant pathological modification of α-synuclein in familial and sporadic Lewy body disease. J Biol Chem 281:29739–29752
3. Appel-Cresswell S, Vilarino-Guell C, Encarnacion M, Sherman H, Yu I, Shah B et al (2013) Alpha-synuclein p.H50Q, a novel pathogenic mutation for Parkinson's disease. Mov Disord 28(6):811–813
4. Arias E, Heron M, Xu J (2017) United States life tables, 2014. Natl Vital Stat Rep 66:1–64
5. Asi YT, Simpson JE, Heath PR, Wharton SB, Lees AJ, Revesz T et al (2014) Alpha-synuclein mRNA expression in oligodendrocytes in MSA. Glia 62(6):964–970
6. Bandres-Ciga S, Diez-Fairen M, Kim JJ, Singleton AB (2020) Genetics of Parkinson's disease: an introspection of its journey towards precision medicine. Neurobiol Dis 137:104782
7. Bartels T, Ahlstrom LS, Leftin A, Kamp F, Haass C, Brown MF et al (2010) The N-terminus of the intrinsically disordered protein α-synuclein triggers membrane binding and helix folding. Biophys J 99(7):2116–2124
8. Bartz JC (2017) Prion strain diversity. In: Prusiner SB (ed) Prion diseases. Cold Spring Harbor Laboratory Press, New York, pp 31–44
9. Berry DB, Lu D, Geva M, Watts JC, Bhardwaj S, Oehler A et al (2013) Drug resistance confounding prion therapeutics. Proc Natl Acad Sci USA 110:E4160–E4169
10. Bertoncini CW, Jung YS, Fernandez CO, Hoyer W, Griesinger C, Jovin TM et al (2005) Release of long-range tertiary interactions potentiates aggregation of natively unstructured alpha-synuclein. Proc Natl Acad Sci USA 102(5):1430–1435
11. Boyer DR, Li B, Sun C, Fan W, Sawaya MR, Jiang L et al (2019) Structures of fibrils formed by α-synuclein hereditary disease mutant H50Q reveal new polymorphs. Nat Struct Mol Biol 26(11):1044–1052
12. Boyer DR, Li B, Sun C, Fan W, Zhou K, Hughes MP et al (2020) The α-synuclein hereditary mutation E46K unlocks a more stable, pathogenic fibril structure. Proc Natl Acad Sci USA 117:3592–3602
13. Braak H, Del Tredici K, Rub U, de Vos RA, Jansen Steur EN, Braak E (2003) Staging of brain pathology related to sporadic Parkinson's disease. Neurobiol Aging 24:197–211
14. Bradford BM, Wijaya CAW, Mabbott NA (2019) Discrimination of prion strain targeting in the central nervous system via reactive astrocyte heterogeneity in CD44 expression. Front Cell Neurosci 13:411
15. Brahmachari S, Ge P, Lee SH, Kim D, Karuppagounder SS, Kumar M et al (2016) Activation of tyrosine kinase c-Abl contributes to α-synuclein-induced neurodegeneration. J Clin Invest 126(8):2970–2988
16. Budka H (2003) Neuropathology of prion diseases. Br Med Bull 66:121–130
17. Burré J, Sharma M, Tsetsenis T, Buchman V, Etherton MR, Südhof TC (2010) Alpha-synuclein promotes SNARE-complex assembly in vivo and in vitro. Science 329(5999):1663–1667
18. Bussell R Jr, Ramlall TF, Eliezer D (2005) Helix periodicity, topology, and dynamics of membrane-associated alpha-synuclein. Protein Sci 14(4):862–872
19. Chandra S, Chen X, Rizo J, Jahn R, Südhof TC (2003) A broken α-helix in folded α-synuclein. J Biol Chem 278:15313–15318
20. Collinge J, Clarke AR (2007) A general model of prion strains and their pathogenicity. Science 318:930–936
21. Davidson WS, Jonas A, Clayton DF, George JM (1998) Stabilization of alpha-synuclein secondary structure upon binding to synthetic membranes. J Biol Chem 273(16):9443–9449
22. Djelloul M, Holmqvist S, Boza-Serrano A, Azevedo C, Yeung MS, Goldwurm S et al (2015) Alpha-synuclein expression in the oligodendrocyte lineage: an in vitro and in vivo study using rodent and human models. Stem Cell Reports 5(2):174–184
23. Domingo E, Perales C (2019) Viral quasispecies. PLoS Genet 15:e1008271
24. Domingo E, Sabo D, Taniguchi T, Weissmann C (1978) Nucleotide sequence heterogeneity of an RNA phage population. Cell 13:735–744
25. Eigen M (1971) Selforganization of matter and the evolution of biological macromolecules. Naturwissenschaften 58:465–523
26. Eliezer D, Kutluay E, Bussell R Jr, Browne G (2001) Conformational properties of alpha-synuclein in its free and lipid-associated states. J Mol Biol 307(4):1061–1073
27. Fares M-B, Ait-Bouziad N, Dikiy I, Mbefo MK, Jovičić A, Kiely A et al (2014) The novel Parkinson's disease linked mutation G51D attenuates *in vitro* aggregation and membrane binding of α-synuclein, and enhances its secretion and nuclear localization in cells. Hum Mol Genet 23:4491–4509
28. Ferreon AC, Gambin Y, Lemke EA, Deniz AA (2009) Interplay of alpha-synuclein binding and conformational switching probed by single-molecule fluorescence. Proc Natl Acad Sci USA 106(14):5645–5650
29. Fevga C, Park Y, Lohmann E, Kievit AJ, Breedveld GJ, Ferraro F et al (2021) A new alpha-synuclein missense variant (Thr72Met) in two Turkish families with Parkinson's disease. Parkinsonism Relat Disord 89:63–72
30. Forster E, Lewy FH (1912) Paralysis agitans. In: Lewandowsky M (ed) Pathologische anatomie handbuch der neurologie. Springer Verlag, New York, pp 920–933
31. Fortin DL, Nemani VM, Voglmaier SM, Anthony MD, Ryan TA, Edwards RH (2005) Neural activity controls the synaptic accumulation of alpha-synuclein. J Neurosci 25(47):10913–10921
32. Fraser H (1979) Neuropathology of scrapie: the precision of the lesions and their diversity. In: Prusiner SB, Hadlow WJ (eds) Slow transmissible diseases of the nervous system, vol 1. Academic Press, New York, pp 387–406
33. Frieg B, Geraets JA, Strohäker T, Dienemann C, Mavroeidi P, Jung BC et al (2021) α-synuclein polymorphism determines oligodendroglial dysfunction. bioRxiv. https://doi.org/10.1101/2021.07.09.451731
34. Ghaemmaghami S, May BCH, Renslo AR, Prusiner SB (2010) Discovery of 2-aminothiazoles as potent antiprion compounds. J Virol 84:3408–3412
35. Ghosh D, Sahay S, Ranjan P, Salot S, Mohite GM, Singh PK et al (2014) The newly discovered Parkinson's disease

associated Finnish mutation (A53E) attenuates α-synuclein aggregation and membrane binding. Biochemistry 53(41):6419–6421
36. Giasson BI, Duda JE, Quinn SM, Zhang B, Trojanowski JQ, Lee VM (2002) Neuronal α-synucleinopathy with severe movement disorder in mice expressing A53T human α-synuclein. Neuron 34:521–533
37. Giasson BI, Murray IV, Trojanowski JQ, Lee VM (2001) A hydrophobic stretch of 12 amino acid residues in the middle of alpha-synuclein is essential for filament assembly. J Biol Chem 276(4):2380–2386
38. Gilman S, Low PA, Quinn N, Albanese A, Ben-Shlomo Y, Fowler CJ et al (1999) Consensus statement on the diagnosis of multiple system atrophy. J Neurol Sci 163:94–98
39. Gilman S, May SJ, Shults CW, Tanner CM, Kukull W, Lee VM-Y et al (2005) The north American multiple system atrophy study group. J Neural Transm (Vienna) 112:1687–1694
40. Gilman S, Wenning GK, Low PA, Brooks DJ, Mathias CJ, Trojanowski JQ et al (2008) Second consensus statement on the diagnosis of multiple system atrophy. Neurology 71:670–676
41. Gokarn YR, Fesinmeyer RM, Saluja A, Razinkov V, Chase SF, Laue TM et al (2011) Effective charge measurements reveal selective and preferential accumulation of anions, but not cations, at the protein surface in dilute salt solutions. Protein Sci 20:580–587
42. Guerrero-Ferreira R, Taylor NM, Arteni AA, Kumari P, Mona D, Ringler P et al (2019) Two new polymorphic structures of human full-length alpha-synuclein fibrils solved by cryo-electron microscopy. Elife 8:e48907
43. Guerrero-Ferreira R, Taylor NM, Mona D, Ringler P, Lauer ME, Riek R et al (2018) Cryo-EM structure of alpha-synuclein fibrils. Elife 7:e36402
44. He S, Scheres SHW (2017) Helical reconstruction in RELION. J Struct Biol 198:163–176
45. Holec SAM, Woerman AL (2020) Evidence of distinct α-synuclein strains underlying disease heterogeneity. Acta Neuropathol 142(1):73–86
46. Hutchinson EG, Thonton JM (1993) The Greek key motif: extraction, classification, and analysis. Protein Eng 6:233–245
47. Jao CC, Der-Sarkissian A, Chen J, Langen R (2004) Structure of membrane-bound alpha-synuclein studied by site-directed spin labeling. Proc Natl Acad Sci USA 101(22):8331–8336
48. Kiely AP, Asi YT, Kara E, Limousin P, Ling H, Lewis P et al (2013) α-synucleinopathy associated with G51D *SNCA* mutation: a link between Parkinson's disease and multiple system atrophy? Acta Neuropathol 125:753–769
49. Koros C, Stamelou M, Simitsi A, Beratis I, Papadimitriou D, Papagiannakis N et al (2018) Selective cognitive impairment and hyposmia in p.A53T SNCA PD vs typical PD. Neurology 90:e864–e869
50. Kruger R, Kuhn W, Leenders KL, Sprengelmeyer R, Muller T, Woitalla D et al (2001) Familial parkinsonism with synuclein pathology: clinical and PET studies of A30P mutation carriers. Neurology 56:1355–1362
51. Krüger R, Kuhn W, Müller T, Woitalla D, Graeber M, Kösel S et al (1998) Ala30Pro mutation in the gene encoding alpha-synuclein in Parkinson's disease. Nat Genet 18(2):106–108
52. Kuzdas-Wood D, Stefanova N, Jellinger KA, Seppi K, Schlossmacher MG, Poewe W et al (2014) Towards translational therapies for multiple system atrophy. Prog Neurobiol 118:19–35
53. Lau A, So RWL, Lau HHC, Sang JC, Ruiz-Riquelme A, Fleck SC et al (2020) α-Synuclein strains target distinct brain regions and cell types. Nat Neurosci 23(1):21–31
54. Lazaro DF, Dias MC, Carija A, Navarro S, Madaleno CS, Tenreiro S et al (2016) The effects of the novel A53E alpha-synuclein mutation on its oligomerization and aggregation. Acta Neuropathol Commun 4(1):128
55. Lesage S, Anheim M, Letournel F, Bousset L, Honoré A, Rozas N et al (2013) G51D α-synuclein mutation causes a novel parkinsonian–pyramidal syndrome. Ann Neurol 73:459–471
56. Lesage S, Brice A (2009) Parkinson's disease: from monogenic forms to genetic susceptibility factors. Hum Mol Genet 18:R48-59
57. Levine PM, Galesic A, Balana AT, Mahul-Mellier AL, Navarro MX, De Leon CA et al (2019) α-Synuclein O-GlcNAcylation alters aggregation and toxicity, revealing certain residues as potential inhibitors of Parkinson's disease. Proc Natl Acad Sci USA 116(5):1511–1519
58. Li B, Ge P, Murray KA, Sheth P, Zhang M, Nair G et al (2018) Cryo-EM of full-length α-synuclein reveals fibril polymorphs with a common structural kernel. Nat Commun 9:3609
59. Li J, Browning S, Mahal SP, Oelschlegel AM, Weissmann C (2010) Darwinian evolution of prions in cell culture. Science 327:869–872
60. Li J, Mahal SP, Demczyk CA, Weissmann C (2011) Mutability of prions. EMBO Rep 12:1243–1250
61. Li Y, Zhao C, Luo F, Liu Z, Gui X, Luo Z et al (2018) Amyloid fibril structure of α-synuclein determined by cryo-electron microscopy. Cell Res 28:897–903
62. Liu H, Koros C, Strohaker T, Schulte C, Bozi M, Varvaresos S et al (2021) A novel SNCA A30G mutation causes familial Parkinson's disease. Mov Disord 36(7):1624–1633
63. Logan T, Bendor J, Toupin C, Thorn K, Edwards RH (2017) α-synuclein promotes dilation of the exocytotic fusion pore. Nat Neurosci 20:681–689
64. Long H, Zheng W, Liu Y, Sun Y, Zhao K, Liu Z et al (2021) Wild-type α-synuclein inherits the structure and exacerbated neuropathology of E46K mutant fibril strain by cross-seeding. Proc Natl Acad Sci USA 118(20):e2012435118
65. Lövestam S, Schweighauser M, Matsubara T, Murayama S, Tomita T, Ando T et al (2021) Seeded assembly *in vitro* does not replicate the structures of α-synuclein filaments from multiple system atrophy. FEBS Open Bio 11(4):999–1013
66. Mahal SP, Baker CA, Demczyk CA, Smith EW, Julius C, Weissmann C (2007) Prion strain discrimination in cell culture: the cell panel assay. Proc Natl Acad Sci USA 104:20908–20913
67. Martikainen MH, Paivarinta M, Hietala M, Kaasinen V (2015) Clinical and imaging findings in Parkinson disease associated with the A53E SNCA mutation. Neurol Genet 1:e27
68. McKeith IG, Boeve BF, Dickson DW, Halliday GM, Taylor JP, Weintraub D et al (2017) Diagnosis and management of dementia with Lewy bodies: fourth consensus report of the DLB Consortium. Neurology 89:88–100
69. McKeith IG, Dickson DW, Lowe J, Emre M, O'Brien JT, Feldman H et al (2005) Diagnosis and management of dementia with Lewy bodies: third report of the DLB consortium. Neurology 65:1863–1872
70. Medda L, Barse B, Cugia F, Bostrom M, Parsons DF, Ninham BW et al (2012) Hofmeister challenges: ion binding and charge of the BSA protein as explicit examples. Langmuir 28:16355–16363
71. Medda L, Carucci C, Parsons DF, Ninham BW, Monduzzi M, Salis A (2013) Specific cation effects on hemoglobin aggregation below and at physiological salt concentration. Langmuir 29:15350–15358
72. Miller DW, Johnson JM, Solano SM, Hollingsworth ZR, Standaert DG, Young AB (2005) Absence of alpha-synuclein mRNA expression in normal and multiple system atrophy oligodendroglia. J Neural Transm 112(12):1613–1624
73. Mohite GM, Kumar R, Panigrahi R, Navalkar A, Singh N, Datta D et al (2018) Comparison of kinetics, toxicity, oligomer formation, and membrane binding capacity of α-synuclein familial

mutations at the A53 site, including the newly discovered A53V mutation. Biochemistry 57(35):5183–5187
74. Narhi L, Wood SJ, Steavenson S, Jiang Y, Wu GM, Anafi D et al (1999) Both familial Parkinson's disease mutations accelerate alpha-synuclein aggregation. J Biol Chem 274(14):9843–9846
75. Nemani VM, Lu W, Berge V, Nakamura K, Onoa B, Lee MK et al (2010) Increased expression of alpha-synuclein reduces neurotransmitter release by inhibiting synaptic vesicle reclustering after endocytosis. Neuron 65(1):66–79
76. Ni X, McGlinchey RP, Jiang J, Lee JC (2019) Structural insights into α-synuclein fibril polymorphism: effects of Parkinson's disease-related C-terminal truncations. J Mol Biol 431(19):3913–3919
77. Nielsen SB, Macchi F, Raccosta S, Langkilde AE, Giehm L, Kyrsting A et al (2013) Wildtype and A30P mutant alpha-synuclein form different fibril structures. PLoS ONE 8(7):e67713
78. Papp MI, Kahn JE, Lantos PL (1989) Glial cytoplasmic inclusions in the CNS of patients with multiple system atrophy (striatonigral degeneration, olivopontocerebellar atrophy and Shy-Drager syndrome). J Neurol Sci 94:79–100
79. Parkinson J (1817) An essay on the shaking palsy. Sherwood, Neely, and Jones, New York
80. Pasanen P, Myllykangas L, Siitonen M, Raunio A, Kaakkola S, Lyytinen J et al (2014) A novel α-synuclein mutation A53E associated with atypical multiple system atrophy and Parkinson's disease-type pathology. Neurobiol Aging 35:2180.e2181-2180.e2185
81. Polymeropoulos MH, Lavedan C, Leroy E, Ide SE, Dehejia A, Dutra A et al (1997) Mutation in the α-synuclein gene identified in families with Parkinson's disease. Science 276:2045–2047
82. Proukakis C, Dudzik CG, Brier T, MacKay DS, Cooper JM, Millhauser GL et al (2013) A novel α-synuclein missense mutation in Parkinson disease. Neurology 80(11):1062–1064
83. Prusiner SB, Woerman AL, Mordes DA, Watts JC, Rampersaud R, Berry DB et al (2015) Evidence for α-synuclein prions causing multiple system atrophy in humans with parkinsonism. Proc Natl Acad Sci USA 112:E5308–E5317
84. Rao JN, Jao CC, Hegde BG, Langen R, Ulmer TS (2010) A combinatorial NMR and EPR approach for evaluating the structural ensemble of partially folded proteins. J Am Chem Soc 132:8657–8668
85. Rodriguez JA, Ivanova MI, Sawaya MR, Cascio D, Reyes FE, Shi D et al (2015) Structure of the toxic core of α-synuclein from invisible crystals. Nature 525:486–490
86. Rosborough K, Patel N, Kalia LV (2017) α-synuclein and Parkinsonism: updates and future perspectives. Curr Neurol Neurosci Rep 17(4):31
87. Rutherford NJ, Giasson BI (2015) The A53E α-synuclein pathological mutation demonstrates reduced aggregation propensity in vitro and in cell culture. Neurosci Lett 597:43–48
88. Rutherford NJ, Moore BD, Golde TE, Giasson BI (2014) Divergent effects of the H50Q and G51D SNCA mutations on the aggregation of α-synuclein. J Neurochem 131(6):859–867
89. Sacino AN, Brooks M, Thomas MA, McKinney AB, McGarvey NH, Rutherford NJ et al (2014) Amyloidogenic α-synuclein seeds do not invariably induce rapid, widespread pathology in mice. Acta Neuropathol 127(5):645–665
90. Salis A, Cappai L, Carucci C, Parsons DF, Monduzzi M (2020) Specific buffer effects on the intermolecular interactions among protein molecules at physiological pH. J Phys Chem Lett 11:6805–6811
91. Scheres SHW (2020) Amyloid structure determination in RELION-3.1. Acta Crystallogr D Struct Biol 76:94–101
92. Schweighauser M, Shi Y, Tarutani A, Kametani F, Murzin AG, Ghetti B et al (2020) Structures of α-synuclein filaments from multiple system atrophy. Nature 585(7825):464–469
93. Shahnawaz M, Mukherjee A, Pritzkow S, Mendez N, Rabadia P, Liu X et al (2020) Discriminating α-synuclein strains in Parkinson's disease and multiple system atrophy. Nature 578(7794):273–277
94. Spillantini MG, Schmidt ML, Lee VM-Y, Trojanowski JQ, Jakes R, Goedert M (1997) α-synuclein in Lewy bodies. Nature 388:839–840
95. Strohaker T, Jung BC, Liou SH, Fernandez CO, Riedel D, Becker S et al (2019) Structural heterogeneity of α-synuclein fibrils amplified from patient brain extracts. Nat Commun 10(1):5535
96. Sun Y, Hou S, Zhao K, Long H, Liu Z, Gao J et al (2020) Cryo-EM structure of full-length α-synuclein amyloid fibril with Parkinson's disease familial A53T mutation. Cell Res 30(4):360–362
97. Sun Y, Long H, Xia W, Wang K, Zhang X, Sun B et al (2021) The hereditary mutation G51D unlocks a distinct fibril strain transmissible to wild-type α-synuclein. Nat Commun 12(1):6252
98. Telling GC, Parchi P, DeArmond SJ, Cortelli P, Montagna P, Gabizon R et al (1996) Evidence for the conformation of the pathologic isoform of the prion protein enciphering and propagating prion diversity. Science 274:2079–2082
99. Tran J, Anastacio H, Bardy C (2020) Genetic predispositions of Parkinson's disease revealed in patient-derived brain cells. NPJ Parkinsons Dis 6:8
100. Tuttle MD, Comellas G, Nieuwkoop AJ, Covell DJ, Berthold DA, Kloepper KD et al (2016) Solid-state NMR structure of a pathogenic fibril of full-length human α-synuclein. Nat Struct Mol Biol 23(5):409–415
101. Uéda K, Fukushima H, Masliah E, Xia Y, Iwai A, Yoshimoto M et al (1993) Molecular cloning of cDNA encoding an unrecognized component of amyloid in Alzheimer disease. Proc Natl Acad Sci USA 90:11282–11286
102. Ulmer TS, Bax A, Cole NB, Nussbaum RL (2005) Structure and dynamics of micelle-bound human alpha-synuclein. J Biol Chem 280(10):9595–9603
103. Vargas KJ, Makani S, Davis T, Westphal CH, Castillo PE, Chandra SS (2014) Synucleins regulate the kinetics of synaptic vesicle endocytosis. J Neurosci 34:9364–9376
104. Vargas KJ, Schrod N, Davis T, Fernandez-Busnadiego R, Taguchi YV, Laugks U et al (2017) Synucleins have multiple effects on presynaptic architecture. Cell Rep 18:161–173
105. Watts JC, Giles K, Oehler A, Middleton L, Dexter DT, Gentleman SM et al (2013) Transmission of multiple system atrophy prions to transgenic mice. Proc Natl Acad Sci USA 110:19555–19560
106. Woerman AL, Kazmi SA, Patel S, Aoyagi A, Oehler A, Widjaja K et al (2018) Familial Parkinson's point mutation abolishes multiple system atrophy prion replication. Proc Natl Acad Sci USA 115:409–414
107. Woerman AL, Kazmi SA, Patel S, Freyman Y, Oehler A, Aoyagi A et al (2018) MSA prions exhibit remarkable stability and resistance to inactivation. Acta Neuropathol 135:49–63
108. Woerman AL, Oehler A, Kazmi SA, Lee J, Halliday GM, Middleton LT et al (2019) Multiple system atrophy prions retain strain specificity after serial propagation in two different Tg(*SNCA**A53T) mouse lines. Acta Neuropathol 137:437–454
109. Wu KP, Weinstock DS, Narayanan C, Levy RM, Baum J (2009) Structural reorganization of alpha-synuclein at low pH observed by NMR and REMD simulations. J Mol Biol 391(4):784–796
110. Yonetani M, Nonaka T, Masuda M, Inukai Y, Oikawa T, Hisanaga S et al (2009) Conversion of wild-type alpha-synuclein into mutant-type fibrils and its propagation in the presence of A30P mutant. J Biol Chem 284:7940–7950

111. Yoshino H, Hirano M, Stoessl AJ, Imamichi Y, Ikeda A, Li Y et al (2017) Homozygous alpha-synuclein p.A53V in familial Parkinson's disease. Neurobiol Aging 57:248
112. Zarranz JJ, Alegre J, Gómez-Esteban JC, Lezcano E, Ros R, Ampuero I et al (2004) The new mutation, E46K, of α-synuclein causes Parkinson and Lewy body dementia. Ann Neurol 55:164–173
113. Zhao K, Li Y, Liu Z, Long H, Zhao C, Luo F et al (2020) Parkinson's disease associated mutation E46K of α-synuclein triggers the formation of a distinct fibril structure. Nat Commun 11:2643
114. Zhao K, Lim YJ, Liu Z, Long H, Sun Y, Hu JJ et al (2020) Parkinson's disease-related phosphorylation at Tyr39 rearranges α-synuclein amyloid fibril structure revealed by cryo-EM. Proc Natl Acad Sci USA 117:20305–20315